Energy Proceedings
Vol 55, 2025
ISSN 2004-2965

System Dynamics Analysis of Interaction Behaviors and Pricing Mechanisms in Grid-Hydrogen-Vehicle System

Ruoxuan Zhao[1], Qiming Yang [2], Gengfeng Li [1*], Minghao Li[1], Chenlin Ji[3], Dafu Liu[1], Ziwen Xu[1], Jiaju Shi[1], Zhaohong Bie[1]

1 State Key Laboratory of Electrical Insulation and Power Equipment (Xi'an Jiaotong University), Xi'an 710049, China

2 Pudong Power Supply Company of State Grid Shanghai Electric Power Co., Ltd., Shanghai 200120, China

3 Wuxi Power Supply Company of State Grid Jiangsu Electric Power Co., Ltd., Wuxi 214061, China

(Corresponding Author: gengfengli@xjtu.edu.cn)

ABSTRACT

As hydrogen energy increasingly permeates the power system, complex relationships emerge among the power grid, hydrogen energy storage (HES), and hydrogen vehicle (HV). These relationships are influenced by numerous factors, necessitating a systematic analysis. This study utilizes system dynamics (SD) to investigate the grid-hydrogen-vehicle interaction process. A causal loop diagram for the grid-hydrogen-vehicle interaction process is constructed, the flow relationships between internal factors within the power grid and hydrogen modules are refined, and an exploration of how price changes affect the interaction process is conducted. Case study analysis demonstrates that the SD model can simulate the dynamic evolution of grid-hydrogen-vehicle interaction. By guiding interaction behaviors through price adjustments, the model can increase benefits for all parties involved, thereby providing an effective method for establishing practical pricing adjustment mechanisms.

Keywords: system dynamics, hydrogen energy storage, hydrogen vehicle, evolution analysis, pricing mechanism

NONMENCLATURE

Abbreviations	
SD	System Dynamics
HES	Hydrogen Energy Storage
HV	Hydrogen Vehicle

1. INTRODUCTION

Recent advances in renewable energy technologies have significantly increased the penetration of intermittent sources like wind and solar power in the energy mix. However, the inherent variability of these sources poses substantial challenges for grid stability and reliability. Hydrogen energy storage (HES) has been proposed as a solution due to their ability to store and release energy on demand. Hydrogen can be produced from excess renewable energy through electrolysis, stored, and then utilized to meet energy demands when renewable generation is low. Additionally, the hydrogen produced can also be transported to refueling stations to supply hydrogen vehicle (HV). HV can also return electricity to the grid during power shortages, thus enabling a beneficial interaction among the power grid, HES, and HV.

There is abundant research on the grid-hydrogen-vehicle interaction process. [1] examines the optimization of hydrogen station placement considering the coupling of distribution networks and hydrogen fuel vehicles, highlighting strategies that balance economic and energy efficiency. [2] explores the planning of wind-hydrogen-electric coupling networks that capture traffic flows, proposing a model that integrates renewable energy sources with hydrogen production and vehicle refueling stations. [3] discusses the economic feasibility of automotive hydrogen refueling stations and long-distance hydrogen transport using offshore wind power, assessing the integration of green hydrogen into automotive applications. [4] proposes an optimal strategy for operating integrated electric power and hydrogen systems using vehicle-based hydrogen transport. [5] focuses on the coordinated planning of electricity and hydrogen networks, integrating a hydrogen supply chain for fuel cell electric vehicles to enhance system flexibility and resilience. [6] develops a framework for planning the expansion of distribution networks integrated with hydrogen refueling stations and renewable energy sources. Existing research primarily focuses on the planning issues related to the interaction among power grid, HES, and HV, but does not specifically analyze the factors influencing the decision-

This is a paper for the 16th International Conference on Applied Energy (ICAE2024), Sep. 1-5, 2024, Niigata, Japan.

making of the three parties involved and their patterns of change.

SD is a methodological framework used to understand the behavior of complex systems over time, involving the study of feedback loops, stocks, and flows to model the interdependencies and dynamics influencing decision-making processes within interconnected systems. There are already some studies applying SD to the hydrogen energy field. [7] explores the use of SD to forecast hydrogen demand in the transportation sector, incorporating various influencing factors and potential changes under different scenarios. [8] presents a long-term forecast of hydrogen demand in China using system dynamics to enhance planning in hydrogen energy systems. However, existing research has only applied SD at the planning level for forecasting hydrogen demand, with no studies exploring its application from the perspective of stakeholders to analyze interaction among power grid, HES, and HV.

The interaction among power grid, HES, and HV is influenced by numerous factors such as fluctuations in renewable energy output, load variability, hydrogen production, and the refueling demands of hydrogen fuel cell vehicle users [9]. Changes in these elements can lead to modifications in decision-making processes across these sectors, which are reflected in shifts in electricity pricing, generation compensation, and hydrogen refueling costs, ultimately affecting the profits of all involved parties [10]. Consequently, the intricate interdependencies among the power grid, HES, and HV sectors highlight the significance of understanding the underlying factors and their patterns of change, which are critical for maximizing benefits and enhancing the synergy within this interaction.

This paper employs SD to investigate the interaction among power grid, HES, and HV. The main contributions are summarized as follows:

• Utilize causal loop analysis to qualitatively depict the complex elements and feedback relationships within the grid-hydrogen-vehicle network, establishing a basis for analyzing the impact of various factors on interactive decision-making.

• Employ flow diagrams to quantitatively analyze the internal structures of modules, uncovering the causal dynamics of the grid-hydrogen-vehicle interaction process.

• Provide an effective methodology for developing pricing mechanisms, offering guidance for formulating interactive incentive measures.

2. CAUSAL LOOP ANALYSIS OF GRID-HYDROGEN-VEHICLE INTERACTION PROCESS

The grid-hydrogen-vehicle interaction process involves the interplay among the power grid, HES, and HV users. Essentially, this process entails the transfer of electrical energy, hydrogen energy, and benefits. In this interactive process, the power grid's electricity pricing strategy influences the hydrogen production of HES [11]. Changes in the hydrogen supply and demand prompt HES operators to adjust the hydrogen selling price, which in turn affects the refueling behavior of HV users. Furthermore, the power grid's generation compensation pricing strategy affects the discharging power of HES and HVs, while the decisions made by HES operators and HV

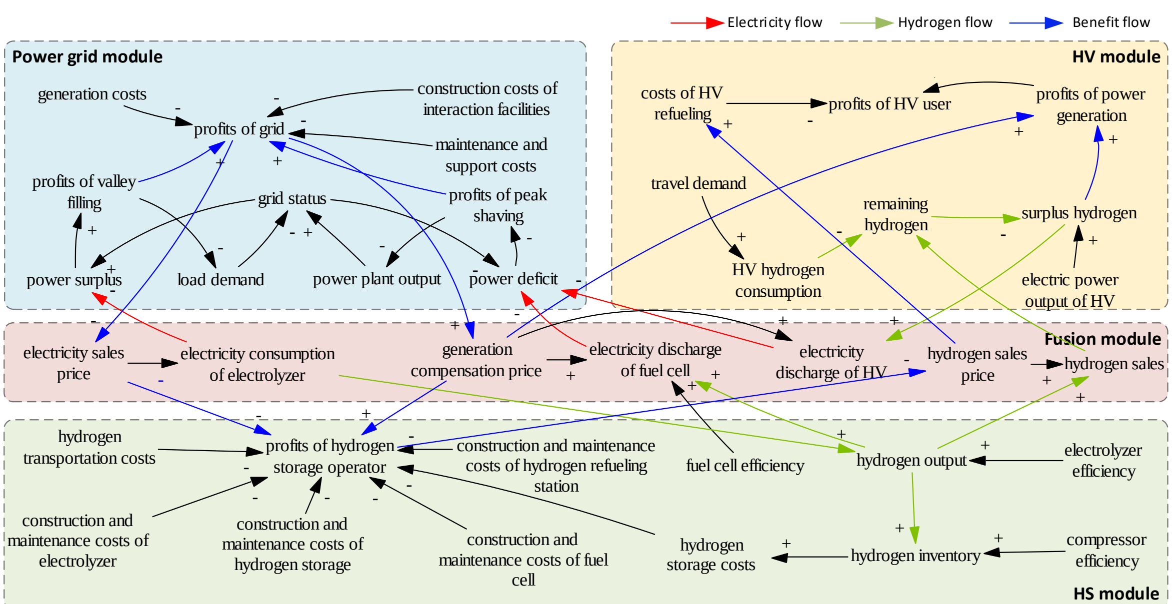

Fig. 1 Grid-Hydrogen-Vehicle Interaction Causal Loop Diagram

users influence the state of the power grid, thereby prompting changes in its pricing strategy. The causal loop diagram qualitatively describes the positive and negative correlations among these factors. The causal loop diagram for the grid-hydrogen-vehicle interaction process is shown in Figure 1.

The causal loop diagram of the grid-hydrogen-vehicle interaction process includes four parts: the power grid module, the HES module, the HV module, and the fusion module. The power grid module adjusts electricity prices and generation compensation prices to guide users' electricity consumption or production, thereby maintaining power balance. The HES module adjusts hydrogen pricing based on hydrogen production and demand. The HV module decides on refueling and discharging behaviors based on its hydrogen storage and price signals. The three parties interact through changes in prices, electricity, and hydrogen quantities in the fusion module, achieving the transfer of electrical energy, hydrogen energy, and benefits. Changes in the profits of the power grid, HES, and HV are also crucial factors affecting their decision-making [12]. As it stands, the various factors involved in the grid-hydrogen-vehicle interaction are numerous, and the decisions within modules and their interconnections are complex [13]. Relying solely on the qualitative analysis of the causal loop diagram does not accurately portray the grid-hydrogen-vehicle interaction process, necessitating more in-depth analysis.

3. SYSTEM DYNAMICS ANALYSIS OF GRID-HYDROGEN-VEHICLE INTERACTION PROCESS

The causal loop diagram of grid-hydrogen-vehicle interaction qualitatively represents the positive and negative relationships within each module as well as the feedback relationships between them. For a more intuitive expression of the system's internal feedback forms and control laws, this section details the internal structure of each module in the interaction using flow diagrams and analyzes the causal dynamics between variables.

3.1 Power Grid Module

Due to load fluctuations and variations in power plant output, the power grid may experience either power surpluses or shortages. HES and HV can provide power absorption or support to the grid. The grid maximizes its operational revenue by adjusting electricity prices and generation compensation prices. Figure 2 shows the flow diagram of power grid module.

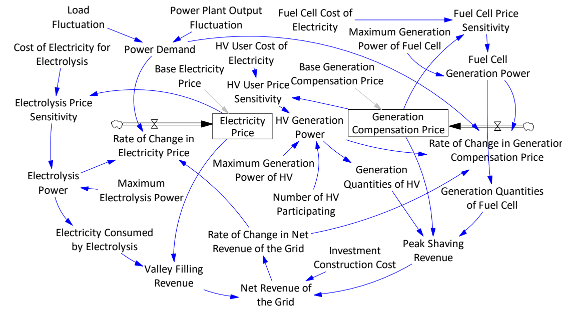

Fig. 2 Flow Diagram of Power Grid Module

The power grid's power demand is affected by fluctuations at the generation and load ends, leading to either power surpluses or shortages. Power demand can be expressed as

$$P_{demand} = \Delta P_{load} - \Delta P_{plant} \tag{1}$$

where a positive value indicates a power shortage and a negative value indicates a power surplus, ΔP_{load} represents load fluctuation, and ΔP_{plant} represents power plant output fluctuation.

During power surpluses, electrolyzers can absorb excess power to produce hydrogen. HES operators adjust the electrolysis power based on the electricity price, defining the price sensitivity of electrolysis as

$$\omega_{el} = 1 - \exp[-\lambda_{el}(E_{el} - E_u)] \tag{2}$$

where λ_{el} is the electrolysis price sensitivity coefficient, E_{el} is the cost of electricity for electrolysis, and E_u is the electricity price.

The electrolysis power can be determined as

$$P_{el} = \omega_{el} P_{el,\max} \tag{3}$$

where $P_{el,\max}$ is the maximum electrolysis power.

The electricity consumed by electrolysis is determined by the electrolysis power and the usage time, represented as

$$W_{el} = P_{el} \Delta T \tag{4}$$

where ΔT is the time interval, set as 0.25 hours in this paper.

Valley filling revenue induced by electricity price can be expressed as

$$R_{con} = W_{el} E_u \tag{5}$$

During power shortages, fuel cells in HES facilities can use hydrogen stored in tanks to generate electricity, and HVs can also supply power to the grid through interaction nodes. The grid guides the generation behavior of HES operators and HV users by adjusting the generation compensation price and ensures maximization of its operational revenue. HV user price sensitivity is defined as

$$\omega_v = 1 - \exp[-\lambda_v(E_v - E_g)] \tag{6}$$

where λ_v is the HV user price sensitivity coefficient, E_v is the cost of electricity for HV users, and E_g is the generation compensation price.

Similarly, fuel cell price sensitivity can be expressed as

$$\omega_{fc} = 1 - \exp[-\lambda_{fc}(E_{fc} - E_g)] \tag{7}$$

where λ_{fc} is the fuel cell price sensitivity coefficient, and E_{fc} is the fuel cell cost of electricity.

The generation power of HV and fuel cell can be calculated as

$$P_v = N_{v,elec}\omega_v P_{v,\max} \tag{8}$$

$$P_{fc} = \omega_{fc} P_{fc,\max} \tag{9}$$

where P_v is the HV generation power, $N_{v,elec}$ is the number of HV participating in the response, $P_{v,\max}$ is the maximum generation power of HV, P_{fc} is the fuel cell generation power, and $P_{fc,\max}$ is the maximum generation power of fuel cell.

The generation quantities of HV and fuel cell can be obtained as

$$W_v = P_v \Delta T \tag{10}$$

$$W_{fc} = P_{fc} \Delta T \tag{11}$$

Peak shaving revenue induced by generation compensation price can be expressed as

$$R_{gen} = (W_v + W_{fc})(E_{loss} - E_g) \tag{12}$$

where E_{loss} is the cost per unit of power deficiency.

The net revenue of the grid within a unit time interval can be represented as

$$R_{grid} = R_{con} + R_{gen} - C_{inv} \cdot \frac{\Delta T}{8760} \tag{13}$$

where C_{inv} is the annual investment construction cost added by the grid to interact with HES and HV.

The rate of change in electricity price is affected by power demand, electrolysis power, and net revenue of the grid, expressed as

$$\Delta E_u = \chi_u \xi_u (1 - \frac{P_{el}}{-P_{demand}})\ln(\mathrm{e} + \frac{dR_{grid}}{dt}) \tag{14}$$

$$\chi_u = \begin{cases} 1, P_{demand} < 0 \\ 0, P_{demand} \geq 0 \end{cases} \tag{15}$$

Where t is the time step for simulation, χ_u is the electricity demand determination sign, and ξ_u is the electricity price change rate adjustment factor.

Due to the responsive process of the grid to adjustments in electricity prices, there is a time delay, represented by a SD time delay function

$$E_u = \int f_{\text{delay1}}(\Delta E_u, t_u)dt + E_{u0} \tag{16}$$

$f_{\text{delay1}}(x, y)$ is the time delay function in SD, where x represents the delayed variable, y represents the delay value, t_u is the time step for adjusting the electricity price, and E_{u0} is the base electricity price.

Similarly, the correction rate of the generation compensation price is influenced by power demand, HV generation power, fuel cell generation power, and net revenue of the grid, expressed as

$$\Delta E_g = \chi_g \xi_g (1 - \frac{P_v + P_{fc}}{P_{demand}})\ln(\mathrm{e} + \frac{dR_{grid}}{dt}) \tag{17}$$

$$\chi_g = \begin{cases} 1, P_{demand} > 0 \\ 0, P_{demand} \leq 0 \end{cases} \tag{18}$$

where χ_g is the generation demand determination sign, and ξ_g is the generation compensation price change rate adjustment factor.

The adjustment of the generation compensation price also has a time delay, represented as

$$E_g = \int f_{\text{delay1}}(\Delta E_g, t_g)dt + E_{g0} \tag{19}$$

where t_g is the time step for adjusting the generation compensation price, and E_{g0} is the base generation compensation price.

3.2 Hydrogen Energy Module

Figure 3 shows the flow diagram of hydrogen energy module. The hydrogen energy module is a combination of the HES module and the HV module, with hydrogen being the main circulating entity in this module. Part of the hydrogen produced by the electrolyzers is used for transportation to refueling stations for sale, meeting the refueling needs of HV users, while another part is stored in hydrogen storage tanks for subsequent transportation or to supply fuel cells for power generation.

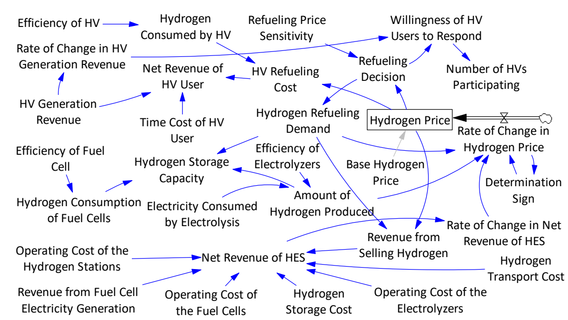

Fig. 3 Flow Diagram of Hydrogen Energy Module

The amount of hydrogen produced can be calculated from the electricity used for electrolysis and the efficiency of the electrolyzers as

$$Q_{h,el} = \sum_{T_{el}} W_{el} / \eta_{el} \tag{20}$$

where T_{el} is the operation duration of the electrolyzers, η_{el} is the efficiency of the electrolyzer.

The hydrogen consumption of the fuel cells can be calculated from the electricity generation of the fuel cells and the efficiency of the fuel cell as

$$Q_{h,fc} = \sum_{T_{fc}} W_{fc} / \eta_{fc} \tag{21}$$

where T_{fc} is the operation duration of the fuel cells, η_{fc} is the efficiency of the fuel cell.

According to consumer psychology, HV users choose to refuel when the hydrogen storage in their vehicle is almost depleted. A small portion of HV users might choose to refuel earlier due to long-distance travel needs. The hydrogen storage pattern of HV can be represented by a truncated normal distribution

$$f(x_v;\mu,\sigma,a,b) = \frac{\frac{1}{\sigma\sqrt{2\pi}}\exp\left(\frac{-(x_v-\mu)^2}{2\sigma^2}\right)}{\Phi(\frac{b-\mu}{\sigma}) - \Phi(\frac{a-\mu}{\sigma})} \tag{22}$$

$$\mu = 0.6,\ \sigma = 0.2,\ a = 0,\ b = 1$$

where x_v is the percentage of hydrogen storage, μ is the mean, σ is the standard deviation, b is the maximum percentage of hydrogen storage, a is the minimum percentage of hydrogen storage, and Φ is the cumulative distribution function of the standard normal distribution.

The refueling price sensitivity of different HV users varies, defined as

$$\omega_r = \delta_r \frac{H_0 - H_r}{H_0} \tag{23}$$

where ω_r is the refueling price sensitivity, H_r is the hydrogen price, H_0 is the base hydrogen price, and δ_r is the refueling price sensitivity coefficient, set as

$$\delta_r = \begin{cases} 0, 0 < x_v < \mu - 2\sigma \\ 2, \mu - 2\sigma < x_v < \mu \\ 0.5, \mu < x_v < 1 \end{cases} \tag{24}$$

Refueling decision are influenced by both the hydrogen price and the remaining hydrogen in the vehicle, defined as

$$Q_r = \gamma(1+\omega_r) \tag{25}$$

Q_r representing the probability of a user refueling within a day, where γ is the decision coefficient, set as

$$\gamma = \begin{cases} 0.7, 0 < x_v < \mu - 2\sigma \\ 0.2, \mu - 2\sigma < x_v < \mu \\ 0.05, \mu < x_v < 1 \end{cases} \tag{26}$$

HV responds to the power demand of the grid by supplying power through interaction nodes and earning revenue, defined as the net revenue of HV user within a unit time interval

$$R_v = R_{v,elec} - C_{v,h} - C_{v,time} \tag{27}$$

$$R_{v,elec} = \frac{W_v E_g}{N_{v,elec}} \tag{28}$$

$$C_{v,h} = \frac{W_v H_r}{\eta_{el} N_{v,elec}} \tag{29}$$

where $R_{v,elec}$ is the HV generation revenue, $C_{v,h}$ is the HV refueling cost, η_v is the efficiency of HV, and $C_{v,time}$ is the time cost per unit time interval for HV user.

Refueling decision affect the hydrogen storage level of HV, influencing the willingness of HV users to respond. Additionally, changes in the revenue of HV user also impact their response willingness, defined as

$$\alpha_v = (1 + \frac{\int (Q_r - \gamma)(1-x_v) f(x;\mu,\sigma,a,b) dx_v}{\int x_v f(x;\mu,\sigma,a,b) dx_v}) \cdot \ln(1 + \frac{dR_v}{dt}) \tag{30}$$

The number of HV participating in the response can be calculated as

$$N_{v,elec} = \alpha_v \beta_v N_v \tag{31}$$

where β_v is the base coefficient for HV participation, N_v is the total number of HV.

Similarly, by estimating the refueling decisions of users, the daily refueling demand can be obtained as

$$D_r = N_v \int Q_r (1-x_v) f(x;\mu,\sigma,a,b) dx_v \tag{32}$$

In the operation segment of the HES operator, the net revenue is influenced by various revenue and cost factors, defined as the daily net revenue of the HES operator

$$\begin{aligned} R_{hsop} = R_{h,sale} + R_{fc,elec} - C_{h,trans} - C_{h,prod} \\ - C_{h,store} - C_{fc,elec} - C_{h,stat} \end{aligned} \tag{33}$$

$$R_{h,sale} = D_r H_r \tag{34}$$

$$R_{fc,elec} = \sum_{T_{fc}} W_{fc} E_g \tag{35}$$

$$C_{h,trans} = c_{trans} D_r \tag{36}$$

$$C_{h,prod} = \sum_{T_{el}} W_{el} E_u + c_{el} Q_{h,el} \tag{37}$$

$$C_{h,store} = c_{store}(Q_{h,el} - D_r - Q_{h,fc}) \tag{38}$$

$$C_{fc,elec} = c_{fc} Q_{h,fc} \tag{39}$$

$$C_{h,stat} = c_{h,stat} D_r \tag{40}$$

where $R_{h,sale}$ is the revenue from selling hydrogen, $R_{fc,elec}$ is the revenue from fuel cell electricity generation, $C_{h,trans}$ is the hydrogen transport cost, c_{trans} is the cost of transporting hydrogen per unit mass, $C_{h,prod}$ is the operating cost of the electrolyzer, c_{el} is the cost of materials, labor, and maintenance per unit mass of hydrogen produced by the electrolyzer, $C_{h,store}$ is the hydrogen storage cost, c_{store} is the storage cost per unit mass of hydrogen, $C_{fc,elec}$ is the operating cost of the fuel cells, c_{fc} is the operating cost per unit mass of hydrogen consumed by the fuel cells, $C_{h,stat}$ is the operating cost of the hydrogen stations, $c_{h,stat}$ is the operational cost of selling hydrogen per unit mass at the hydrogen stations.

The rate of change in the refueling hydrogen price is influenced by the refueling demand and the net revenue of the HES operator, defined as

$$\Delta H_r = \chi_{hsop} \xi_r \left(\frac{Q_{h,el}}{D_r} - 1\right) \tag{41}$$

$$\Delta R_{hsop} = \frac{dR_{hsop}}{dt} \tag{42}$$

$$\chi_{hsop} = \begin{cases} 1, \Delta R_{hsop} > 0 \\ 0, \Delta R_{hsop} \le 0 \end{cases} \tag{43}$$

where ξ_r is the rate of change in the net revenue of the HES operator, ΔR_{hsop} is the hydrogen price change rate adjustment factor, χ_{hsop} is the HES operator revenue change rate determination sign.

Due to the responsive process of the HES operator to adjustments in the refueling hydrogen price, there is a time delay, represented as

$$H_r = \int f_{\text{delay1}}(\Delta H_r, t_h) dt + H_0 \tag{44}$$

where t_h is the time step for hydrogen price adjustment, H_0 is the base hydrogen price.

4. CASE STUDY ANALYSIS

This study selects a region with high penetration of renewable energy as an example, where wind and solar power serve as the primary energy sources. The region is equipped with HES, which includes electrolyzers, hydrogen storage tanks, fuel cells, and a hydrogen refueling station operated by HES operator. The grid's generation compensation incentive measures can influence the region and its surrounding area, affecting ten thousand HVs. Based on the causal feedback relationships of the grid-hydrogen-vehicle interaction process described earlier, the relationships among various variables are inputted into Vensim software to construct a SD model of the electricity-hydrogen interaction process. The constants are assigned as shown in Table 1.

Table 1 Values of simulation parameters

Power grid module				Hydrogen energy module			
Parameter	Value	Parameter	Value	Parameter	Value	Parameter	Value
λ_{el}	20	$P_{fc,\max}$	2MW	T_{el}	19h	c_{trans}	4.2 CNY /kg
E_{el}	0.4CNY /kWh	E_{loss}	10 CNY /kWh	η_{el}	50kWh /kg	c_{el}	7.5 CNY /kg
$P_{el,\max}$	5MW	C_{inv}	30000	T_{fc}	5h	c_{store}	2.4 CNY /kg
ΔT	15min	ξ_u	0.01	η_{fc}	18kWh /kg	c_{fc}	1.3 CNY /kg
λ_v	10	t_u	1	H_0	50 CNY /kg	$c_{h,stat}$	2.7 CNY /kg
E_v	5 CNY /kWh	E_{u0}	0.4 CNY /kWh	η_{el}	16kWh /kg	ξ_r	0.1
λ_{fc}	10	ξ_g	0.05	$C_{v,time}$	2.5	t_h	1
E_{fc}	5 CNY /kWh	t_g	1	β_v	0.05	H_0	50 CNY /kg
$P_{v,\max}$	7 kW	E_{g0}	5 CNY /kWh	N_v	10000		

From Figure 4, data on typical daily wind and solar power output and load demand in this area show clear power surpluses and deficits during peak and off-peak periods, respectively. This case introduces a price change mechanism to improve the power surpluses and deficits, using this data as input for the power grid module.

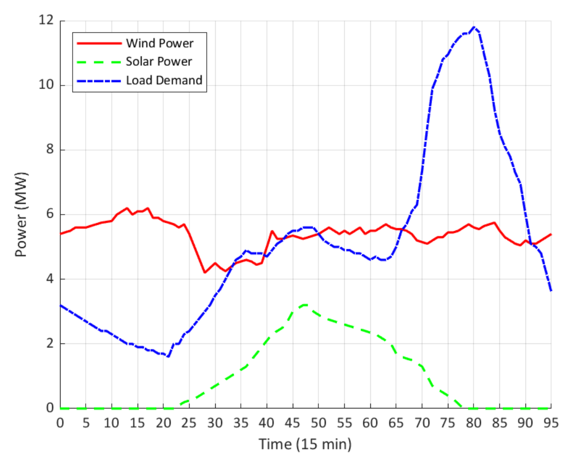

Fig. 4 Daily Power Output and Load Demand

The simulation time is set at 3:30 AM, at which point the system has a surplus power of 4MW. The grid lowers the electricity price to guide the electrolyzers to consume electricity for valley filling.

Figure 5 shows that as the electricity price decreases, both the power of the electrolyzers and the valley filling revenue increase, and their rates of change gradually decrease until they stabilize at zero, indicating that the simulation has found the optimal electricity price for maximizing grid valley filling revenue at this moment.

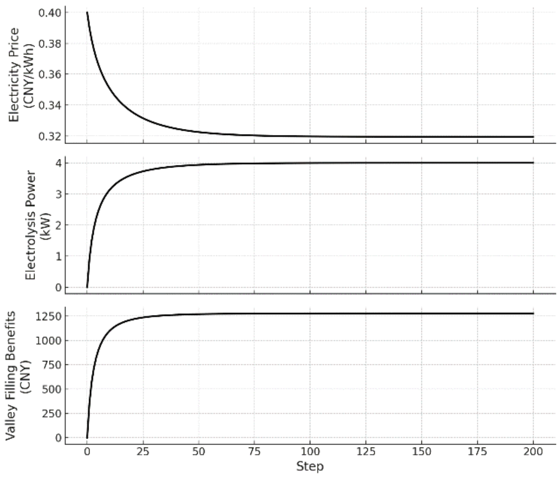

Fig. 5 Change Curve of Electricity Price, Electrolysis Power and Valley Filling Revenue

The simulation time is set at 7:30 PM, at which point the system has a power deficit of 6MW. The grid raises the electricity compensation price to guide HV users and fuel cells to generate power for peak shaving.

Figure 6 reveals that as the generation compensation price decreases, the power output of HVs, fuel cells, and peak shaving revenue all increase, and their rates of change gradually decrease until they stabilize at zero, indicating that the simulation has found the optimal generation compensation price for maximizing grid peak shaving revenue at this moment.

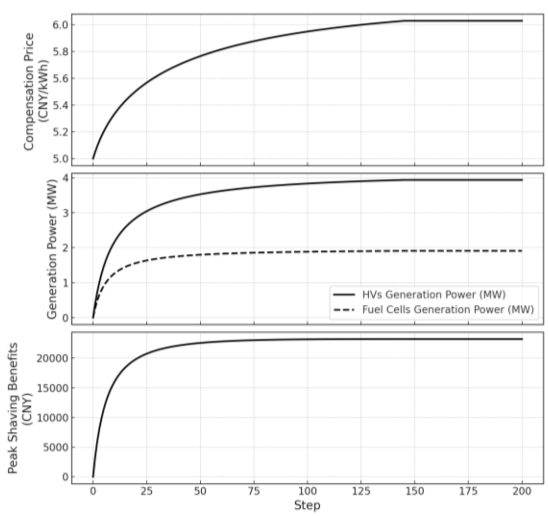

Fig. 6 Change Curve of Compensation Price, Generation Power and Peak Shaving Revenue

Under the revision mechanisms of electricity and generation compensation prices established in this paper, the simulation captures the daily pattern of electricity price changes, as well as the power variations of the electrolyzers, HVs, and fuel cells.

Figures 7 and 8 show that when the grid has power surpluses, the electricity price is inversely proportional to the surplus power value; and when there is a power deficit, the generation compensation price is directly proportional to the deficit power value, confirming that the price correction mechanism aligns with objective laws.

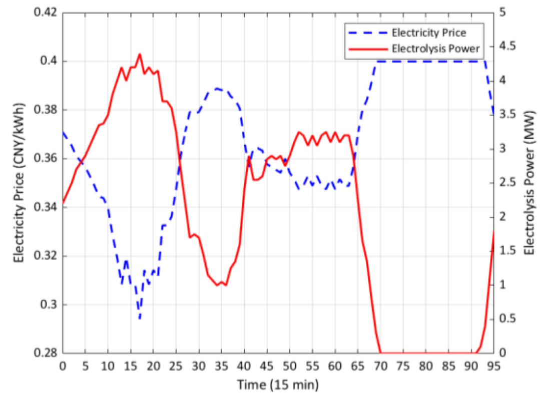

Fig. 7 Daily Electricity Price and Electrolysis Power

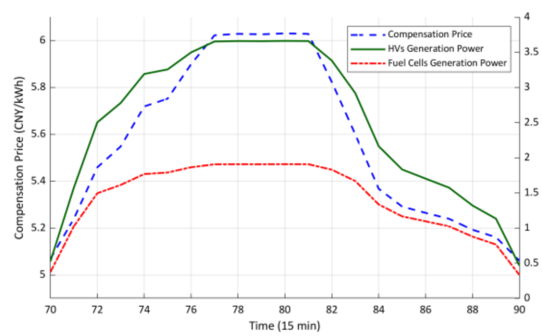

Fig. 8 Daily Compensation Price and Generation Power

Based on the simulation results of the electricity grid module, the daily electricity consumption of the electrolyzers, as well as the power generation of HVs and fuel cells, can be calculated and used as inputs for the HES module. Assuming an average daily refueling demand at the hydrogen station of 414kg, a hydrogen price change mechanism is introduced. The HES operator adjusts the hydrogen price based on hydrogen production, influencing the change in refueling demand and thereby enhancing its own revenue. The simulation results show the changes in hydrogen price, refueling demand, and hydrogen sales revenue for the day.

Figure 9 indicates that as the hydrogen price decreases, the demand for hydrogen gradually increases, suggesting that the reduction in price enhances the refueling willingness of HV users. The rate of increase in hydrogen sales revenue gradually decreases until it stabilizes at zero, indicating that the optimal hydrogen selling price for maximizing daily sales revenue has been achieved.

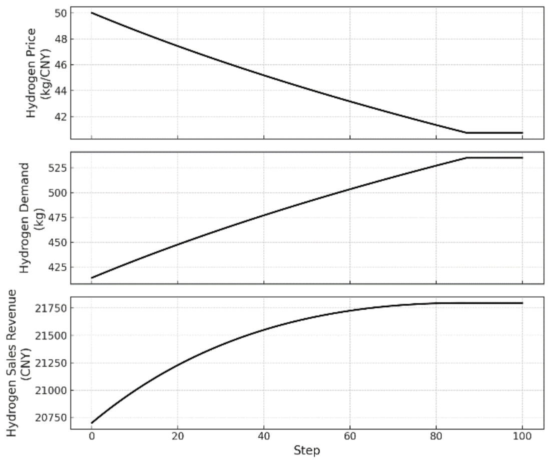

Fig. 9 Change Curve of Hydrogen Price, Hydrogen Demand and Hydrogen Sales Revenue

Table 2 displays the changes in revenue for all parties and the HV response rate before and after the introduction of the pricing mechanisms.

Table 2 Changes in introduction of pricing mechanisms

	Net Revenue/CNY			HV Response
	Grid	HES	HV Users	Rate
Before	-235,056.2	6,458.4	0	5%
After	-108,482.9	34,500.5	58.91	6.446%
Change	126,573.3	28,042.1	58.91	1.446%

It can be seen that the introduction of the pricing mechanism significantly enhances the revenues of the grid-hydrogen-vehicle triad and also increases the willingness of HV users to participate in responses.

5. CONCLUSIONS

This study builds a SD model to understand the interconnected effects among factors in the grid-hydrogen-vehicle interaction process, analyzing the impact of these factors and their feedback relationships. The conclusions are as follows:

(1) The interaction involves multiple factors with complex relationships. The causal analysis loop effectively outlines the complex elements and their interrelations, serving as a basis for analyzing how each factor influences decisions within the system.

(2) Detailed flowcharts of the modules, including the power grid and hydrogen energy modules, facilitate a quantitative analysis of the causal dynamics among the variables.

(3) Vensim-based SD case analysis shows that decisions within grid-hydrogen-vehicle interaction evolve dynamically, which can inform the development of pricing adjustment mechanisms for grid-hydrogen-vehicle interaction.

By leveraging the interaction logic and pricing guidance mechanisms derived from this study, grid companies and HES operators can adjust price signals based on real-time operational data. This approach enhances HV users' willingness to participate in generation response, thereby maximizing stakeholder benefits and optimizing resource utilization.

REFERENCE

[1] Huang W, Deng M, Ge L, et al. Layout optimization strategy of hydrogen production and refueling stations considering the coupling effect of distribution network and hydrogen fuel vehicles. High Voltage Engineering 2023, 49 (01): 105-117.

[2] Jiang Y, Yang G, Zhu Z. Wind-hydrogen-electricity coupled network planning considering traffic flow capture 2021, 45 (22): 19-28.

[3] Zhang H, Pan J, He B, et al. Economic analysis of automobile hydrogen refueling station and long-distance hydrogen energy transportation based on offshore wind power. Advanced Technology of Electrical Engineering and Energy 2023, 42 (08): 50-59.

[4] Shao C, Feng C, Shahidehpour M, et al. Optimal stochastic operation of integrated electric power and renewable energy with vehicle-based hydrogen energy system. IEEE Transactions on Power Systems 2021, 36(5): 4310-4321.

[5] Tao Y, Qiu J, Lai S, et al. Coordinated planning of electricity and hydrogen networks with hydrogen supply chain for fuel cell electric vehicles. IEEE Transactions on Sustainable Energy 2022, 14(2): 1010-1023.

[6] Tabandeh A, Hossain M J, Li L. Integrated multi-stage and multi-zone distribution network expansion planning with renewable energy sources and hydrogen refuelling stations for fuel cell vehicles. Applied Energy 2022, 319: 119242.

[7] Zhou Z, Miao S, Yuan T. Prediction of hydrogen demand in transportation field based on system dynamics. Electric Power Automation Equipment 2024, 44 (04): 33-39+47.

[8] Yuan T, Zhang Y, Yang Z, et al. Medium and long-term hydrogen load prediction based on system dynamics. Electric Power 2023, 56 (10): 11-21.

[9] Yang Q, Li G, Bie Z, et al. Coordinated power supply restoration method of resilient urban transmission and distribution networks considering intermittent new energy. High Voltage Engineering 2023, 49(07): 2764-2774.

[10] Yang Q, Li G, Bie Z, et al. Vehicle-to-grid based resilience promotion strategy for urban distribution network under typhoon disaster. Automation of Electric Power Systems 2022,46(12):130-139.

[11] Yang Q, Ji C, Liu Y, et al. Day-rolling optimization strategy for photovoltaic-energy storage charging station with multiple electric bus lines. Smart Power,2020,48(8):44-50,90.

[12] Yang Q, Ji C. Intraday Rolling Optimization Strategy of PV-Energy Storage-Integrated Charging Station Serving Multiple Electrical Bus Lines. 2020 5th Asia Conference on Power and Electrical Engineering (ACPEE). IEEE, 2020: 1143-1149.

[13] Ji C, Yang Q, Ning N, et al. Mitigating Downward Reserve Deficiency of Power System via Coordinating EV Demand Response at Valley Period. IEEE Access, 2020, 8: 112368-112378.